PERGAMON

International Journal of Heat and Mass Transfer 41 (1998) 3149–3156

International Journal of HEAT and MASS TRANSFER

Transient cooling of water around a cylinder in a rectangular cavity—a numerical analysis of the effect of the position of the cylinder

K. Sasaguchi[a,*], K. Kuwabara[a], K. Kusano[b], H. Kitagawa[c]

[a] *Department of Mechanical Engineering, Kumamoto University, 2-39-1 Kurokami, Kumamoto City 860, Japan*
[b] *Department of Mechanical Engineering, Tokushima University, Tokushima 770, Japan*
[c] *Kyushu Electric Power Company Inc., Fukuoka 810, Japan*

Received 17 March 1997; in final form 12 January 1998

Abstract

This paper reports the effect of the position of a cooled cylinder in a rectangular cavity on the cooling process of water around the cylinder. The governing equations are solved by a finite difference method, and the flow structure and temperature distributions are predicted. The initial water temperature, T_i, is varied at 4, 6, 8 and 12°C, while the temperature of the cylinder surface is fixed at 0°C. The obtained timewise variations of the temperature field and the velocity field as well as the mean Nusselt number over the cylinder surface are compared. The changes in the position of the cylinder and the initial water temperature largely affect fluid flows. Only an upward flow appears along the cylinder for $T_i = 4$°C, while for $T_i > 4$°C a downward flow is observed in early stages, and then the flow direction is changed to upward. Therefore, an averaged Nusselt number over the cylinder surface and averaged water temperature vary in a complicated manner with time for $T_i > 4$°C. The cooling rate of water is largely affected by the change of the position of the cylinder.

Nomenclature

a thermal diffusivity
c specific heat
d diameter of the cylinder
$\mathbf{g}$ gravitational acceleration vector
$\bar{h}$ averaged heat transfer coefficient over the cylinder surface
Nu mean Nusselt number over the cylinder surface
n outward normal to the cylinder surface
Pr Prandtl number, ν/a
p pressure
q see eqn. (4)
$\bar{q}$ averaged heat flux over the cylinder surface
Ra Rayleigh number, $\rho_{max} g\omega d^3 (T_i - T_w)^q/\rho a\nu$
T temperature
$\bar{T}$ average water temperature
t time
$\mathbf{u}$ velocity vector
X, Y dimensionless coordinate axes, x/d, y/d
x, y coordinate axes (see Fig. 2)
$(\bar{\ })$ average value.

Greek symbols
λ thermal conductivity
ν kinematic viscosity
θ dimensionless temperature $(T-T_i)/(T_w-T_i)$
$\bar{\theta}$ dimensionless area averaged temperature, $(\bar{T}-T_i)/(T_w-T_i)$
ξ, η transformed coordinate axes (see Fig. 2)
ρ density
ρ_{max} see eqn. (4)
τ dimensionless time, at/d^2
ω see eqn. (4).

Subscripts
i initial
ref reference value at $(T_w + T_i)/2$
w cylinder surface.

* Corresponding author. E-mail: sasa@gpo.kumamoto-u.ac.jp.

0017-9310/98 $19.00
PII: S0017-9310(98)00064-7

1. Introduction

A number of studies have been reported on sensible heat and latent heat thermal energy storage, since the effective load leveling of electric power at night is an urgent issue today. In those storage systems, water is commonly used as a working fluid because of its inexpensive and nontoxic nature. Therefore, understanding of transient cooling process of water is very important in designing the storage systems. The density inversion of water between 0°C and 4°C complicates fluid flows and heat transfer in the systems. Many experimental and numerical studies [1–6] have reported on the effects of the density inversion of water on the natural convection. Most of these studies deal with steady heat transfer in a rectangular enclosure whose opposing two horizontal or two vertical walls are set at different temperatures. Only a little attention [7] has been focused on the transient heat transfer. However, understanding of the transient natural convection heat transfer is inevitable for practical applications of thermal energy storage. Therefore, extensive study on it is needed, especially on the transient heat transfer in water around cylinders in a confined region because such configuration commonly appears in many thermal energy storage systems.

The ultimate aim is to clarify transient natural convection around a tube bundle in a confined region. However, as a first step the authors have studied a single cylinder in a rectangular cavity. Recently, we performed a numerical analysis [8] to examine the effect of the initial temperature of water on transient natural convection in water around a cooled cylinder placed at the centre of a rectangular cavity. It was found that the fluid flow and the heat transfer change with time in a complicated way for the initial temperature greater than 4°C.

In the present study, we examined further the effect of the position of the cooled cylinder in the rectangular cavity on transient natural convection in water with the density inversion, since no studies appear to have been reported, to the authors' knowledge. It seems that the position of a cylinder in a cavity greatly affects the cooling process of water due to the density inversion. Therefore, clarification of the effect is important for thermal energy storage. The initial water temperature ranged from 4°C to 12°C, and timewise variations of velocity and temperature fields, averaged Nusselt number over the cylinder surface, as well as the mean water temperature were compared.

2. Physical/numerical model and governing equations

Figure 1 shows the physical system. It consists of a rectangular cavity which contains a horizontal cylinder with diameter d, and all the walls (left, right, top and bottom walls) are assumed to be insulated. In order to examine the effect of the position of the cylinder on the cooling process of water, the position of the cylinder is changed at an upper portion, at the centre and at a lower portion of the cavity, as shown in Fig. 1(a)–(c), respectively. The value of d is arbitrarily set at 0.015 m, and the height and width of the enclosure are also arbitrarily set without considering a particular device, as shown in Fig. 1. The cavity is filled with water. Initially, water is set at a uniform temperature, T_i. At time $t = 0$ s, the temperature of the cylinder surface, T_w, is suddenly changed and maintained at 0°C, and the cooling of water is initiated. Calculations are performed for T_i of 4, 6, 8 and 12°C.

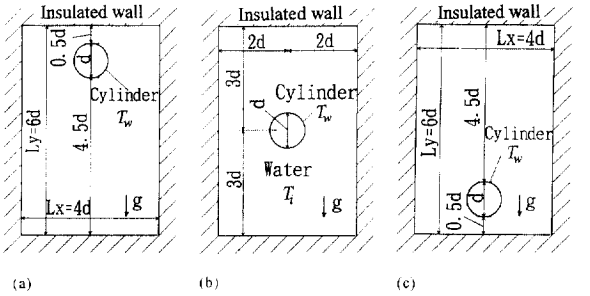

Fig. 1. Physical model: (a) upper-cylinder-case; (b) centered-cylinder-case; (c) lower-cylinder-case.

For simplicity, the following assumptions are made in the analysis: (1) the flow is two-dimensional, laminar and incompressible; (2) the liquid density varies only in the buoyancy term, i.e., water is the Boussinesq liquid. With these assumptions, the dimensional governing equations may be derived as follows:

Continuity

$$\nabla \cdot \mathbf{u} = 0. \tag{1}$$

Momentum

$$\rho \frac{\partial \mathbf{u}}{\partial t} + \rho(\mathbf{u} \cdot \nabla)\mathbf{u} = -\nabla p + \rho \nu \Delta \mathbf{u} + (\rho_{ref} - \rho)\mathbf{g}. \tag{2}$$

Energy equation

$$\rho c \frac{\partial T}{\partial t} + \rho c(\mathbf{u} \cdot \nabla)\mathbf{T} = \lambda \Delta \mathrm{T}. \tag{3}$$

The following density-temperature relationship of water proposed in reference [9] was adopted for the liquid density, ρ,

$$\rho = \rho_{\max}(1 - \omega|T - T_{\max}|^q) \tag{4}$$

where $\rho_{\max} = 999.972$ kg/m^3, $\omega = 9.297173 \times 10^{-6}$ °C^{-q}, $T_{\max} = 4.0293$°C and $q = 1.894816$. This relationship takes into account the nature of the density-inversion in water, and it is introduced to the third term on the right-hand side of equation (2).

Introduction of the Cartesian coordinate system (x–y system) into a complicated physical domain requires

interpolation of the variables, i.e. velocities, temperature and pressure, on some boundaries since the grids are not necessarily coincident with them. To eliminate the errors and complexity due to this interpolation, the governing equations are transformed into a generalized coordinate system, and calculations are performed on the transformed plane. In addition to transforming the governing conservation equations into the generalized coordinate system, it is necessary to adapt the grid lines in the generalized coordinate system to the physical boundaries of the system by properly generating the grids in the physical domain. In the present study, we adopted a numerical grid-generation technique proposed in ref. [10]. A complete set of the dimensionless governing equations and the transformed equations to the generalized coordinate system can be seen in references [8, 11]. Two dimensionless parameters appear in the dimensionless governing equations, namely Rayleigh number, Ra, and Prandtl number, Pr (see NOMENCLATURE for the definitions). The value of Ra is 1.84×10^4, 4.08×10^4, 7.22×10^4 and 1.65×10^5 with a cylinder diameter d, of 0.015 m, and Pr is 12.5, 12.1, 11.7 and 10.9 for $T_i = 4$°C, 6°C, 8°C and 12°C, respectively. All thermophysical properties are evaluated at $(T_i+T_w)/2$.

As an example, Figs 2(a) and 2(b) show the grid system generated by using the technique described above. Fig. 2(b) represents the grid system in the computational plane, and Fig. 2(a) shows the transformed grid from the computational plane into the physical plane. Points indicated by the numbers in the physical and computational planes correspond with each other. Points 1, 3 and 13 in Fig. 2(a) all represent the top of the cylinder surface. In this study, we chose a $81(\xi)\times301(\eta)$ uniform mesh for $T_i = 4$°C and a $81(\xi)\times201(\eta)$ uniform mesh for $T_i > 6$°C in the computational plane, and 0.025-0.2s for time increment. Comparing numerically obtained temperature fields with experimental ones, the validity of the numerical model and the computer code was checked in ref. [8]. The effect of the number of meshes on numerical results was also examined, and Fig. 3 for $T_i = 8$°C with the cylinder located at the lower part of the cavity (Fig. 1(c)) exemplifies the results. In Fig. 3, timewise variations of an averaged Nusselt number over the cylinder surface, $\overline{Nu}$, defined by the next expression,

$$\overline{Nu} = \frac{\bar{h}\cdot d}{\lambda}, \tag{6}$$

where

$$\bar{h} = \frac{\bar{q}}{T_w - T_i} = \frac{\overline{\lambda\left(\frac{\partial T}{\partial n}\right)_w}}{T_w - T_i},$$

are shown. It is seen that $81(\xi)\times201(\eta)$ mesh is adequate for $T_i = 8$°C with the cylinder located at the lower part of the cavity. The same result is obtained for other positions of the cylinder and for $T_i > 4$°C, but 81×301 mesh is used for $T_i = 4$°C because more accurate results are obtained with it than other mesh.

In addition, we can check the accuracy of the calculations with an overall energy balance expressed by the next relation:

$$\left|\bar{\theta} - \frac{\pi}{24-\frac{\pi}{4}}\int_0^{\tau}\overline{Nu}\,d\tau\right| / \bar{\theta} = R \tag{5}$$

where $\bar{\theta}$ is a dimensionless average water temperature over the area which contains water in the cavity. If the energy balance is accomplished, the value of R disappears. However, since there are numerical errors in the calculations there exist some amount of residual. In the present calculations, the maximum value of R among all calculations is 0.12 at $\tau = 6.35$. This value is not so small, but we chose the mesh size and the time increment men-

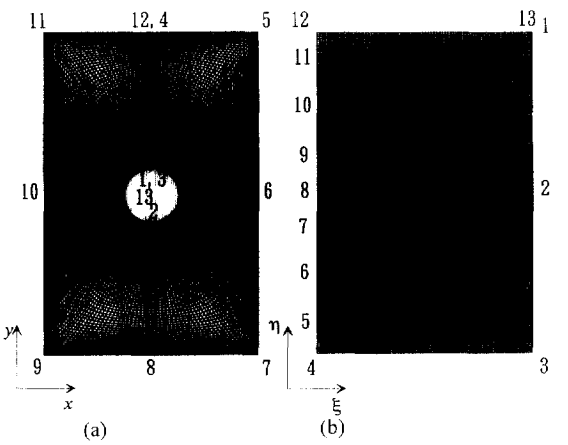

Fig. 2. Grid system : (a) physical plane ; (b) computational plane.

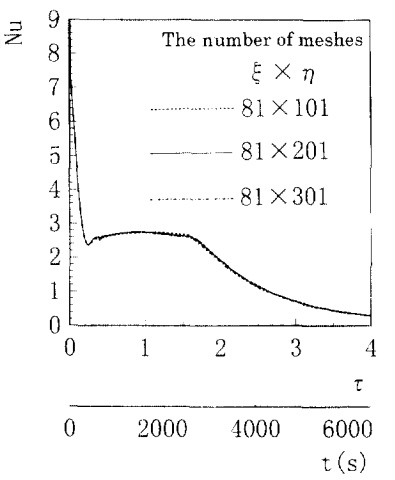

Fig. 3. Check of mesh dependence for $T_i = 8$°C with a cylinder located at a lower part of the cavity as shown in Fig. 1(c).

tioned before with compromise between computational time and accuracy.

The governing equations in the generalized coordinate system were discretized based on the MAC algorithm [12], and they were solved iteratively. Detailed numerical procedure is given in refs. [8, 11].

3. Results and discussion

3.1. Results for $T_i = 4$ C

In order to examine the effect of the position of the cylinder for an initial water temperature, T_i, of 4°C, comparison of temperature distributions at $\tau = 0.870 (t = 1440$ s) are shown in Fig. 4. The density of water increases with temperature in the range between 0°C and 4°C (the density inversion); therefore, for $T_i = 4$°C only an upward flow arises along the cylinder surface at which the temperature is 0°C. As is seen in Fig. 4(a), with the cylinder located in the upper portion of the cavity (the upper-cylinder-case) the upward flow already disappears at $\tau = 0.870$ because the amount of hot water above the cylinder is so small that the temperature difference between the cylinder surface and water above the cylinder decreases very quickly. Thermal stratification has been formed in water under the cylinder, and the heat transfer is almost dominated by conduction. For the case with the cylinder located at the centre of the cavity (the centered-cylinder-case), the upward flow is still observed at this time (Fig. 4(b)) and water above the cylinder is effectively cooled. The upward flow is much stronger at early stages for the case with the lower cylinder (the lower-cylinder-case) than that for the other cases. Cooling of water above the cylinder is accomplished faster for the lower-cylinder-case than that for the centred-cylinder-case. Therefore, only a weak upward flow is observed at $\tau = 0.870$ in Fig. 4(c), but water in the entire region is already cooled down well for the lower-cylinder-case.

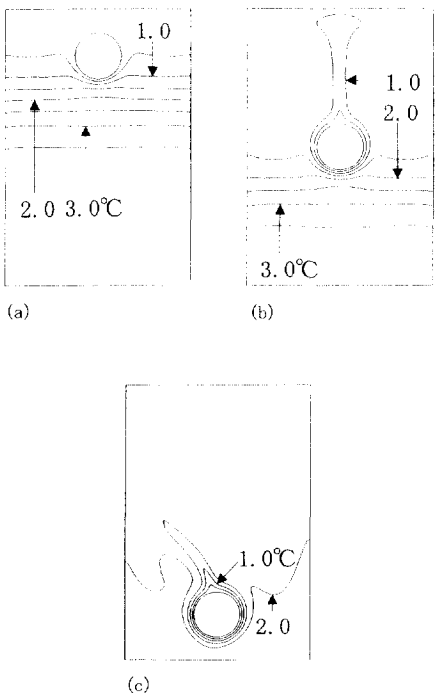

Fig. 4. Comparison of temperature fields at $\tau = 0.870$ ($t = 1440$ s) for $T_i = 4$°C: (a) upper-cylinder-case; (b) centered-cylinder-case; (c) lower-cylinder-case.

Comparison of timewise variations of the average Nusselt number, $\overline{Nu}$, over the cylinder surface is shown in Fig. 5 for $T_i = 4$°C. As described before, for $T_i = 4$°C the upward flow at early stages decays with time, regardless of the position of the cylinder. Accordingly, the average Nusselt number, $\overline{Nu}$, monotonically decreases with time ($\overline{Nu}$ is infinity at $\tau = 0$), as shown in Fig. 5. In particular, the decreasing rate is very large at early stages for the upper-cylinder-case because the upward flow ceases quickly as described before, and the conduction dominated heat transfer lasts for a long period.

Figure 6 shows comparison of timewise variations of a nondimensional averaged water temperature, $\bar{\theta} (= (\bar{T} - T_i)/(T_w - T_i))$, where $\bar{T}$ is an averaged water temperature over the area in the cavity. The value of $\bar{\theta}$ becomes unity when water in the entire region is completely cooled down to T_w. As seen from Fig. 6, $\bar{\theta}$ for the lower-cylinder-case considerably increases with time at early stages, and the value is much larger than those for the other cases. This is because for the lower-cylinder case the large amount of water above the cylinder is effectively cooled down by the strong upward flow at

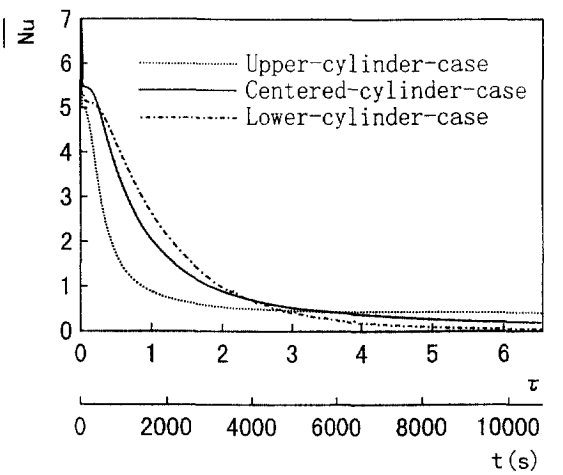

Fig. 5. Timewise variations of averaged Nusselt number over the cylinder surface for $T_i = 4$°C.

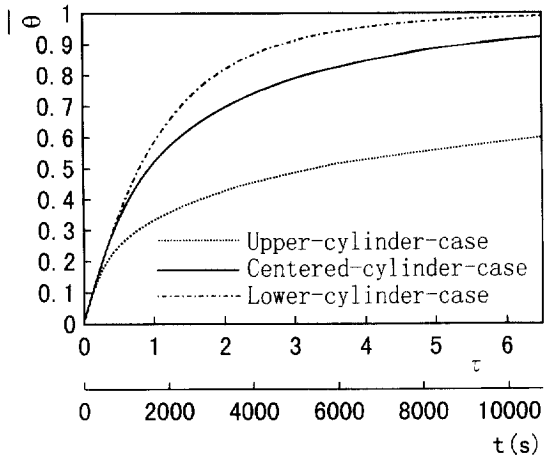

Fig. 6. Timewise variations of averaged water temperature for $T_i = 4°C$.

early periods. On the other hand, for the upper-cylinder-case the decrease in the temperature of water below the cylinder is quite slow so that the increasing rate of $\bar{\theta}$ is very small, except at very early periods.

3.2. *Results for* $T_i = 8°C$

When the initial water temperature is 8°C, the fluid flow and the temperature field become much more complicated since the maximum water density (at ≈4°C) is located at the mid-point between the temperature of the cylinder surface and T_i. Figures 7, 8 and 9 show the timewise variation of the temperature field for the upper-, centred- and lower-cylinder cases, respectively. The timewise variations of $\overline{Nu}$ and $\bar{\theta}$ are shown in Figs 10 and 11, respectively. For the upper-cylinder case (Fig. 7) a strong downward flow arises at an early time (Fig. 7(a)), and then it becomes weak with time due to reduction of the temperature difference between the cylinder surface and water below the cylinder (Fig. 7(b)). An upward flow along the cylinder appears when the temperature of water around the cylinder decreases to around 4°C. However, this upward flow exists only for a short period because the amount of water above the cylinder is very little for the upper-cylinder-case, thus the temperature difference between the cylinder and the water above the cylinder is quickly decreased. As time proceeds further (Fig. 7(c)), almost no natural convection is observed, thermal stratification is established below the cylinder, and the cooling rate of water is considerably reduced. Thus, the value of $\overline{Nu}$ for the upper-cylinder-case decreases almost consistently with time as shown in Fig. 10, and the increasing rate of $\bar{\theta}$ significantly reduces for $\tau > 1.0$ (Fig. 11).

For the centred-cylinder-case (Fig. 8), only a downward flow is evident at an early stage (Fig. 8(a)), as for

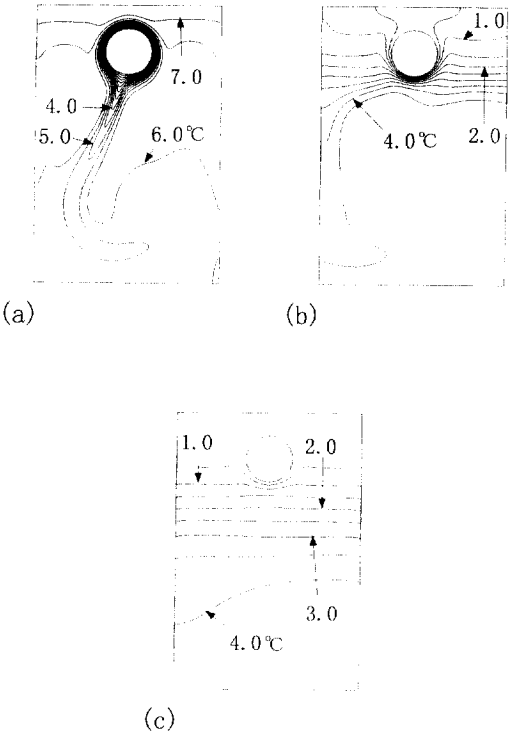

Fig. 7. A timewise variation of temperature field for the upper-cylinder-case for $T_i = 8°C$: (a) $\tau = 0.292$ ($t = 480$ s); (b) $\tau = 1.023$ ($t = 1680$ s); (c) $\tau = 2.484$ ($t = 4080$ s).

the upper-cylinder-case (Fig. 7(a)) since the region where $T > 4°C$ is much larger than that where $T < 4°C$ (the density-inversion region). Water below the cylinder is effectively cooled to nearly 4°C by this strong downward flow. However, the flow becomes weaker as the cooled water with $T \approx 4°C$ accumulates around the cylinder, and the upward force, derived by light water with $T < 4°C$ near the cylinder, gradually increases its strength. Ultimately, it produces in an upward flow along the cylinder, as shown in Fig. 8(b). During the development of the upward flow, almost no flow is observed below the cylinder and the water temperature is kept at nearly 4°C. As time proceeds further, the strength of the upward flow is reduced with a decrease in the water temperature above the cylinder. Finally, heat transfer is almost dominated by conduction (Fig. 8(c)). In Fig. 10, the slight increase in the value of $\overline{Nu}$ during 600 s–1800 s for the centered-cylinder-case is due to the strengthening of the upward flow with time as described above. It is also seen from Fig. 11 that this upward flow suppresses the decrease in the increasing rate of $\bar{\theta}$ as was shown for upper-cylinder-case, thus the increasing rate of $\bar{\theta}$ for the centered-cylinder-case continues to be larger for a longer period in the centered-cylinder-case than it is in the upper-cylinder-case.

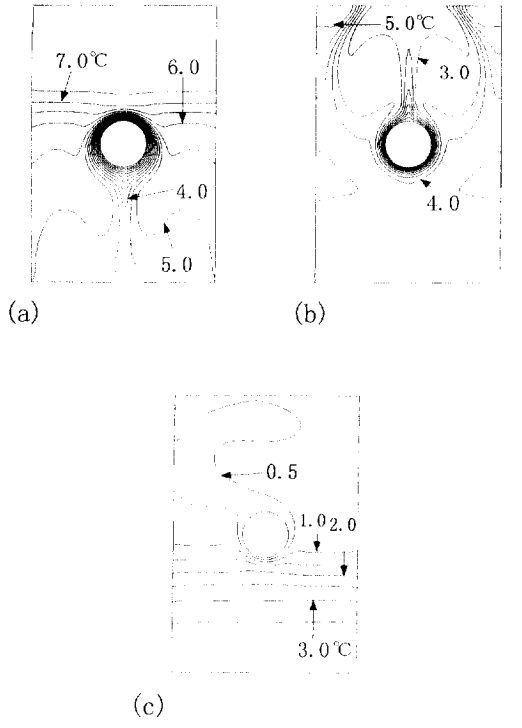

Fig. 8. A timewise variation of temperature field for the centered-cylinder-case for $T_i = 8$ C: (a) $\tau = 0.292$ ($t = 480$ s); (b) $\tau = 1.023$ ($t = 1680$ s); (c) $\tau = 2.484$ ($t = 4080$ s).

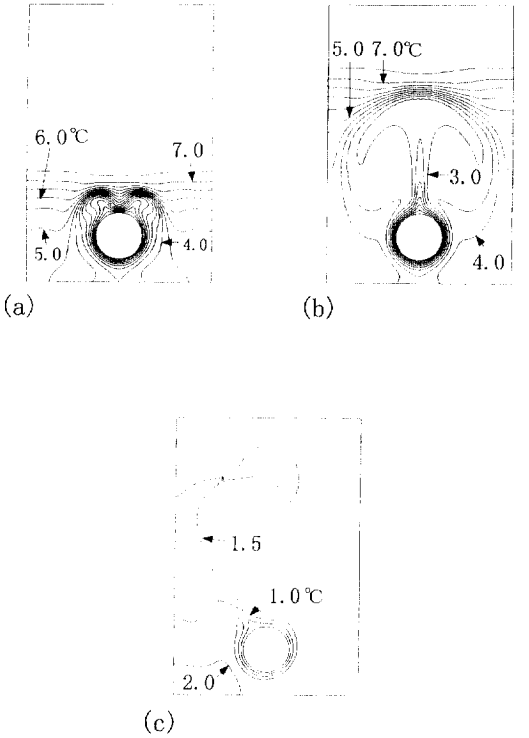

Fig. 9. A timewise variation of temperature field for the lower-cylinder-case for $T_i = 8$ C: (a) $\tau = 0.292$ ($t = 480$ s); (b) $\tau = 1.023$ ($t = 1680$ s); (c) $\tau = 2.484$ ($t = 4080$ s).

For the lower-cylinder-case, as is seen in Fig. 9, an upward flow is predominant almost the entire time range (a downward flow along the cylinder surface is observed for a very short period from the beginning of the cooling process). Water above the cylinder is effectively cooled down for a long period due to this upward flow. Hence, in Fig. 10, the period in which the value of Nu slightly increase is longer for the lower-cylinder-case than that for the centered-cylinder-case, and the value for the lower-cylinder-case remains large even at late stages, compared with the other positions of the cylinder. As is seen from Fig. 11, the value of $\bar{\theta}$ for the lower-cylinder-case is smaller than that for the other cases at early stages since natural convection is stronger for the other cases than that for the lower-cylinder-case. However, at late stages, the value for the lower-cylinder-case exceeds that for other cases because of the long duration of the upward flow in the lower-cylinder-case.

In the case with $T_i = 6$ C (not shown here), an upward flow emerges earlier than in the case with $T_i = 8$ C for all positions of the cylinder. The timewise variations of Nu are qualitatively similar to those with $T_i = 8$ C, but the values of $\bar{\theta}$ vary with time similarly to those with $T_i = 4$ C since the period in which the downward flow exists is very short.

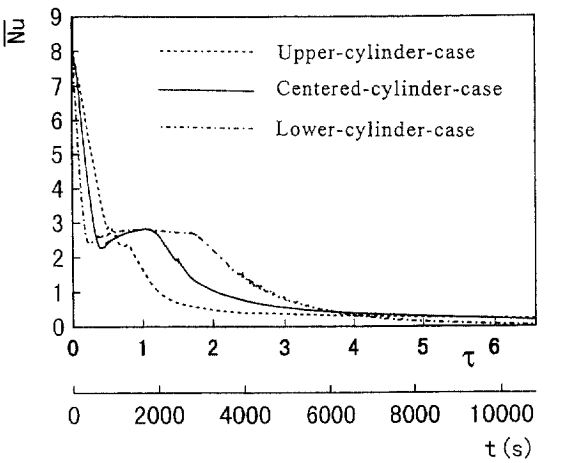

Fig. 10. Timewise variations of averaged Nusselt number on the cylinder surface for $T_i = 8$ C.

3.3. Results for $T_i = 12$ C

For the largest initial-temperature ($T_i = 12$ C) examined in this study, the timewise variation of fluid flow is also similar to that for $T_i = 8$ C. Thus, from Figs 12 and

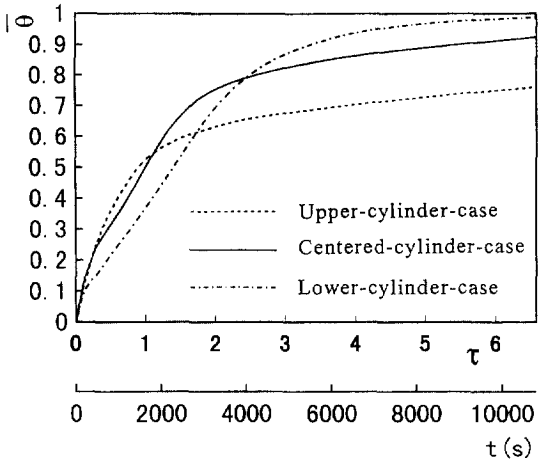

Fig. 11. Timewise variations of averaged water temperature for $T_i = 8$ C.

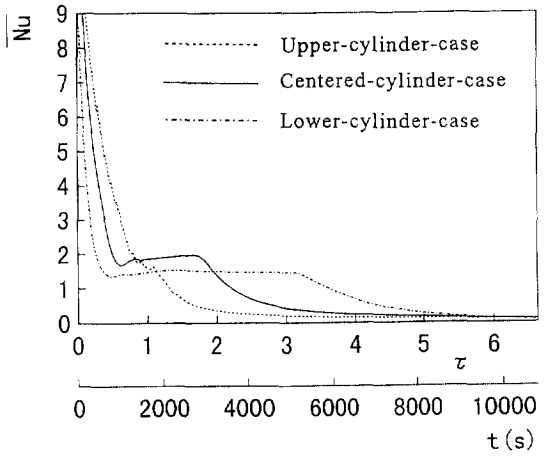

Fig. 12. Timewise variations of averaged Nusselt number on the cylinder surface for $T_i = 12$ C.

13, the variations of $\overline{Nu}$ and $\bar{\theta}$ with time are also similar to those with $T_i = 8°C$ in Figs 10 and 11. However, as is seen in Fig. 14, for the lower-cylinder-case the thermal stratification in water above the cylinder is quite strong so that the development of an upward flow is largely delayed and cooling rate of water remains small for a long period (compare with the case for $T_i = 8°C$ in Fig. 9). As a result, the value of $\overline{Nu}$ for the lower-cylinder-case is smaller than that for the other cases at early stages (Fig. 12). But, as described above, the period in which the upward flow exists is quite long, thus the value of $\overline{Nu}$ remains almost constant for a long period for the lower-cylinder-case and the value becomes greater than that for the other cases at late stages (Fig. 12). This trend reflects the variation of $\bar{\theta}$ with time in Fig. 13, that is, the value of $\bar{\theta}$ for the lower-cylinder-case is much smaller than that

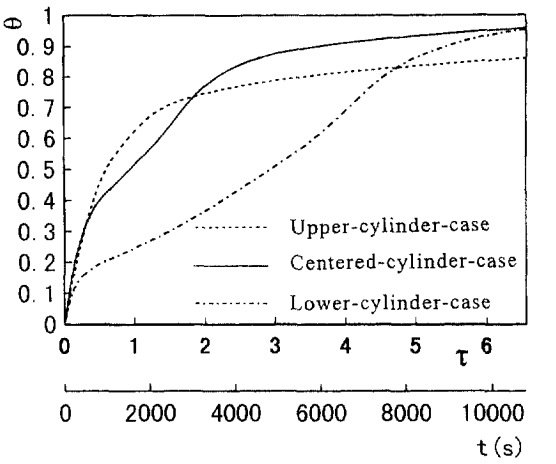

Fig. 13. Timewise variations of averaged water temperature for $T_i = 12$ C.

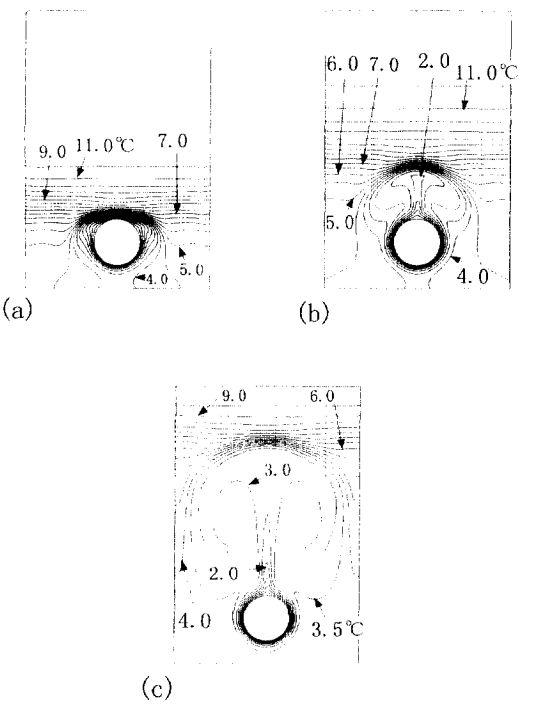

Fig. 14. A timewise variation of temperature field for the lower-cylinder-case for $T_i = 12$ C. (a) $\tau = 0.437$ ($t = 720$ s); (b) $\tau = 1.748$ ($t = 2880$ s); (c) $\tau = 3.642$ ($t = 6000$ s).

for the other cases for a long period from the beginning of cooling, but the difference gradually becomes small with time and almost disappears at around $\tau = 6$.

Distinct asymmetry of temperature fields with respect to a vertical plane through the cylinder axis is found (e.g. see Fig. 7), in spite of the fact that the symmetry in

the geometry, in the temperature and velocity boundary conditions, as well as in the mesh system is secured. It seems that under some conditions a transient flow is so unstable as to create the asymmetrical flow even with small numerical disturbances such as a truncation error in the calculation with double precisions variables. This asymmetry seems to appear also in a real system because disturbances must exist in it, and we should confirm it by very careful experiments in the near future.

4. Conclusions

Numerical calculations were performed to examine the effect of the position of a cooled cylinder in a rectangular cavity on the transient cooling of pure water around the cylinder. The cylinder was placed at an upper portion, the centre, or a lower portion of the cavity (Fig. 1). The initial temperature, T_i, was changed at 4, 6, 8 and 12°C, while the temperature of the cylinder surface was fixed at 0°C.

For $T_i = 4$°C, only an upward flow emerges around the cylinder for all the positions of the cylinder (this flow exists only a short period in the case with the cylinder located at the upper part of the cavity). The upward flow becomes weaker as time proceeds. Hence, the average Nusselt number, Nu, over the cylinder surface decreases consistently with time. The cooling rate of water is the largest with the cylinder located at the lower part of the cavity (the lower-cylinder-case), medium with the cylinder at the centre of the cavity (the centred-cylinder-case), and smallest with the cylinder at the upper part of the cavity (the upper-cylinder-case).

For $T_i > 4$°C, a downward flow is predominated at early stages (this flow exists only for a short period for the lower-cylinder-case). When water around the cylinder is cooled down to nearly 4°C, the flow direction is reversed and an upward flow appears. The upward flow weakens with time as the temperature difference, between the cylinder and water above the cylinder, decreases (this flow exists only for a short period for the upper-cylinder-case). Therefore, the values of Nu and $\bar{\theta}$ vary in a complicated manner with time, as shown in Figs 10, 11, 12 and 13. In addition, for the lower-cylinder-case with $T_i = 12$°C, a strong thermal stratification in water above the cylinder is formed so that the development of the upward flow is largely delayed and the cooling rate is suppressed for a long period (Fig. 13).

In this study, we performed calculations only for an enclosure with a specific height ($6d$) and width ($4d$) as well as for a specific diameter, d ($=0.015$ m), of a cylinder, as shown in Fig. 1. If we consider a different enclosure and cylinder, the feature of natural convection may change and therefore the cooling rate of water may be affected. The authors will conduct numerical simulations to examine these subjects in the near future.

References

[1] Seki N et al. Free convection heat transfer with density inversion in a confined rectangular vessel. Wärme- und Stoffübertragung 1978;11:145–56.
[2] Lin DS, Nansteel MW,. Natural convection heat transfer in a square enclosure containing water near its density maximum. International Journal of Heat and Mass Transfer 1987;30:2319–29.
[3] Braga SL, Viskanta R. Transient convection of water near its density extremum in a rectangular cavity. International Journal of Heat and Mass Transfer 1992;35:861–75.
[4] Ishikawa M et al. Heat transfer correlations of natural convection with density inversion in a vertical enclosure. Transactions of the JSME (in Japanese) 1993;59:564–70.
[5] Tong W, Koster JN. Density inversion effect on transient natural convection in a rectangular enclosure. International Journal of Heat and Mass Transfer 1994;37:927–38.
[6] McDonough MW, Faghri A. Experimental and numerical analyses of the natural convection of water through its density maximum in a rectangular enclosure. International Journal of Heat and Mass Transfer 1994;37:783–801.
[7] Narumi A et al. Cooling and freezing processes of water with a supercooled region in the double horizontal concentric cylinders. Transactions of the JSME (in Japanese) 1990;56:2077–84.
[8] Sasaguchi K et al. Effect of density inversion on cooling of water around a cylinder in a rectangular cavity. Numerical Heat Transfer Part A 1997;32:131–147.
[9] Gebhart B, Mollendorf J. Buoyancy-induced flows in water under conditions in which density extrema may arise. Journal of Fluid Mechanics 1978;89:673–707.
[10] Thompson JF et al. TOMCAT-A code for numerical generation of boundary-fitted curvilinear coordinate systems on fields containing any number of arbitrary two-dimensional bodies. Journal of Computational Physics 1977;24:274–302.
[11] Kitagawa H. Transient natural convection of water around a cylinder in a rectangular cavity. M.S.thesis (in Japanese). Kumamoto University, Japan, 1996.
[12] Takemoto Y. Nakamura Y. Three-dimensional incompressible flow solver. Lecture Notes in Physics. Springer-Verlag 1986;264:594–9.